# Long-term changes in human mobility responses to COVID-19-related information in Japan

Shinya Fukui[*,†]

**Abstract**

This study investigates how human mobility has changed in the long term in response to COVID-19-related information in Japan. We use publicly available daily data on each Japanese prefecture from Google on 'human mobility for retail and recreation' and 'residential spent time'. These can be explained mainly by the number of COVID-19-infected cases, whether a state of emergency was declared, and the vaccination rate. We use the interactive effects model in estimation to control for unobservable human mobility factors that vary over time and have different loadings on a cross-sectional unit. The results show that Japanese citizens were generally fearful of an unknown virus in the first wave; however, they gradually habituated themselves to similar infection information in the subsequent waves. Nevertheless, the level of habituation decreased in view of information regarding new variants that were different from the previous ones. Furthermore, citizens showed heterogeneous responses between the increasing and decreasing phases of infection. Besides, we confirm the spatial interactions of infection information. We also find that vaccination promotion motivated people to venture out of their residences. When considering policy implementation during the pandemic, it is essential to consider information dissemination given: people's habituation, timing, and effective vaccination promotion.

Keywords: COVID-19, Human mobility response, Habituation, Spatial interaction, Vaccination, Interactive effects model

[*] Corresponding author.

[†] Graduate School of Economics, Osaka Metropolitan University, 1-1 Gakuen-cho, Nakaku, Sakai, Osaka 599-8531, Japan. E-mail: shinya.fukui.econ@gmail.com

## 1 Introduction

The COVID-19 pandemic has had significant global socio-economic impacts, including Japan [1, 2]. Given that the transmission of the severe acute respiratory syndrome coronavirus 2 (SARS-CoV-2) can occur through direct or indirect contact with an infected person [3], human mobility (which increases the opportunities for human-to-human contact) can promote the spread of COVID-19 infection [4, 5]. Hence, non-pharmaceutical interventions (NPIs), such as lockdowns, were employed to reduce COVID-19 infections [6-13]. Additionally, when the infection spreads, people restrict their own outgoing behaviour to avoid risks, reducing human mobility [14–16]. For example, from March to May 2020, in the U.S., customer visits fell by 60%; 7% of which was explained by lockdowns, and the rest by own travel restrictions, owing to fear of infection [15]. From these perspectives, it is evident that human mobility and COVID-19 infection are interrelated and have a negative relationship [17].

Human behaviour changes in response to COVID-19-related information are of great concern regarding controlling COVID-19 transmission and the socio-economic impact. Throughout the COVID-19 pandemic, people have essentially been exposed to two main pieces of information: the increase in COVID-19 infections and NPIs [18–21]. Several studies thus explore the behavioural variations in response to COVID-19-related information over time. For example, using data from 124 countries, one study [22] observes a gradual decline in adherence to social distancing under the continued NPIs from March to December 2020. Additionally, Japanese citizens gradually reduced their self-imposed stay-at-home measures despite the infection-increasing phase in 2020 [19, 23]. Furthermore, regarding the declaration of a state of emergency (DSE), an NPI issued between 2020 and 2021 in Japan, other studies [24, 25] find that the extent of curtailment of going-out behaviours slowly decreased from the first to the fourth DSE.

Against the spread of COVID-19 infection, the Japanese government issued the first COVID-19 DSE on 7 April 2020 [26]. Since then, Japan has experienced six waves of COVID-19 infection (as of July 2022) [27], and the government has issued four DSEs [28]. In the first wave, most Japanese citizens feared the unknown virus and the unprecedented widespread pandemic [29]. Since then, Japan has rolled out a rapid vaccination programme [30]. Additionally, the development of therapeutic agents was started worldwide [31], while much more has become known about post-infection effects [32]. Nonetheless, new variants have emerged. However, many individuals have grown tired of the COVID-19 pandemic, exhibiting the so-called ‘pandemic fatigue’ [22]. Therefore, although Japan has experienced the Omicron variant and its subvariant

with a much faster infection rate [33, 34], it is also true that people are slowly becoming accustomed to living with COVID-19. However, the human behavioural changes in response to COVID-19-related information over the long term, over almost three years, are still under-researched. Long-term analysis is thus crucial for future evidence-based policymaking (EBPM) during the pandemic.

Our study uses publicly available human mobility data and analyses how COVID-19-related information affects its variation. First, we explore whether people have become habituated to infection-related information after six waves over two and half years by examining the variation in human mobility in response to COVID-19 infection information. Habituation [35, 36] refers to the diminishing reaction to a repeated stimulus over time [37]. For instance, a study [38] using individual questionnaires shows that COVID-19 anxiety became habituated over sixteen months.

Meanwhile, a single wave of infection comprises an increasing and decreasing phase. Basically, people are less likely to go out in the increasing phase, while in the decreasing phase, they gradually resume going out. However, the more fear people experience, the more inhibited and cautious they behave in either phase, and this behaviour might differ between the two phases. Thus, human mobility responses are considered heterogeneous across the two phases. We validate this conjecture for the first time by identifying the start, end, and peak of infection of different waves in each prefecture in Japan. Moreover, several studies have noted the importance of considering regional spatial interaction when investigating the impact of COVID-19 infection [39, 40]. We examine the spatial interactions between prefectures using cross-prefecture travel to illustrate that information from other prefectures influences the changes in human mobility in one prefecture. As such, we incorporate a cross-term using a spatial weight matrix representing the spatial interactions between prefectures, which has not been done in previous related studies.

Besides, the vaccination would reduce the fear of infection and promote going-out behaviours [41]. The impact of vaccination on human behaviour has only been analysed in one empirical study [42], in which a slight increase in individual travel distance after vaccination is observed but not statistically tested. The impact of multiple DSEs on human behaviour will also need to be re-examined. Moreover, since unobservable factors also affect human mobility, we use the interactive effects model [43] in our regression analysis to control for the unobservable factors that change over time and are accompanied by loadings that differ among cross-sectional units.

While this study does not directly examine individual attitudes, it indirectly explores the changes in fears, risk awareness, and 'pandemic fatigue' through their responses to COVID-19-related information over time and assesses how human mobility responses change over the long-term during a pandemic.

## 2 Data

Our study focuses on three pieces of publicly available COVID-19-related information that affect human mobility: COVID-19-infected cases, DSE (NPI), and vaccination rate.

### *2.1 Human mobility*

The daily human mobility data for each prefecture used in this study are obtained from Google's COVID-19 Community Mobility Reports [44], which are composed of six human mobility categories: *retail & recreation*, *grocery & pharmacy*, *parks*, *transit stations*, *workplaces*, and *residential*; from these, we select *retail & recreation* and *residential*. When avoiding unnecessary mobility, either in reducing the risk of infection or responding to the DSE by the government, people minimise their outings mainly to retail stores (not grocery stores and pharmacies, which are essential) and entertainment venues and also have a greater tendency to stay at home. In Google's data, *residential* indicates time spent at home.

The data show the percentage change compared to a day-of-the-week baseline calculated based on median values for each day of the week for the five weeks from 3 January to 6 February 2020—just prior to the global outbreak of the COVID-19 pandemic. Since these values have day-of-week fluctuations (i.e. each day of the week has its variation characteristics, such as large variations on weekends), we take the difference from the previous week (percentage points) of the percentage change from the baseline. Additionally, by taking the week-on-week difference, rather than using the percentage change from the baseline itself, we can capture the effect of new information in the short term, such as a week-on-week change in the number of daily newly infected cases, on people's decision about whether to go out. An example of a dependent variable is shown in Fig. 1. We denote this dependent variable as $\Delta y_{it}$, where $i = 1, 2, \cdots, N$ stands for the prefecture, $t = 1, 2, \cdots, T$ is the index of day, and $\Delta$ is the difference from the previous week.

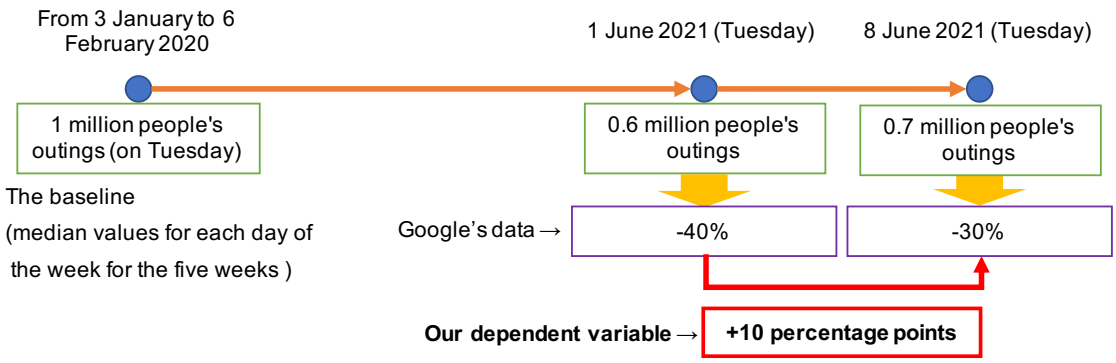


**Figure 1.** Example of a dependent variable for which the author created fake data for the baseline, 1 June 2021 (the previous week), and 8 June 2021.

### *2.2 Infected cases of COVID-19*

Data on the daily number of newly infected cases of COVID-19 are obtained from NHK (*NIPPON HOSO KYOKAI*; Japan Broadcasting Corporation) [45]. Given that the number of new cases fluctuates over a vast range, it is better to take the logarithm of the data to mitigate heteroscedasticity. However, as the data contain zeroes, this is not possible (since the logarithm of zero is undefined). Instead, we use an inverse hyperbolic sine (IHS) transformation, which converts zeros to zeros and behaves similarly to a logarithm [15, 18, 23]. Let $I_{it}$ denote new cases; then, the IHS transformation of $I_{it}$; $I_{it}^*$ becomes

$$I_{it}^* = \ln\left(I_{it} + \sqrt{I_{it}^2 + 1}\right).$$

Additionally, since new cases have day-of-week fluctuations (e.g. fewer PCR tests on weekends), we convert the IHS transformation of new infections to the difference from the same day of the previous week. Hence, the week-on-week difference of daily new infected cases transformed by the IHS, $\Delta I_{it}^*$, approximates the growth rate of new cases compared to the previous week.

Another implication of considering the week-on-week difference is described in the Supplementary Information (Appendix A). Briefly, people tend to judge the severity of COVID-19 infection conditions primarily based on the change in the number of infections from the prior week, as announced in the daily news.

### *2.3 The declaration of a state of emergency*

The DSE data are obtained from the Cabinet Secretariat's COVID-19 Information and Resources [28]. The timing of DSEs varied between prefectures. We set a dummy variable, $E_{it}$, which takes 1 if a DSE is declared in a prefecture and 0 otherwise. The Supplementary Information (Appendix B) displays DSE periods for each prefecture (Fig. S1), while the NPIs in Japan and the contents of the DSE are described in Appendix C.

### *2.4 Vaccination rates*

The daily data on COVID-19 vaccination of each prefecture are obtained from the COVID-19 Vaccination Status by the Digital Agency [46]. We convert the data into a cumulative format to determine the vaccination rate per million persons. Population data for each prefecture (on 1 October 2020) are obtained from Population Estimates by the Statistics Bureau of Japan [47]. Since the number of vaccinations has day-of-week fluctuations, the data (vaccination rate per million persons) are converted to the week-on-week change, denoted by $\Delta V_{it}$.

Other reasons for using the week-on-week change value are provided in the Supplementary Information, Appendix D. In brief, in terms of COVID-19-related information, the larger the increase in the vaccination rate compared to the previous week, the greater the number of people who got vaccinated and formed antibodies; presumably, they become more comfortable going out compared to the previous week.

### *2.5 Time series plots*

The time series plots of variables used in the estimation are shown in Fig. 2. From the figure, infections and human mobility are moving in opposite directions. Further, the first and second vaccinations proceeded rapidly. Additionally, the timing of the DSE differs by prefecture.

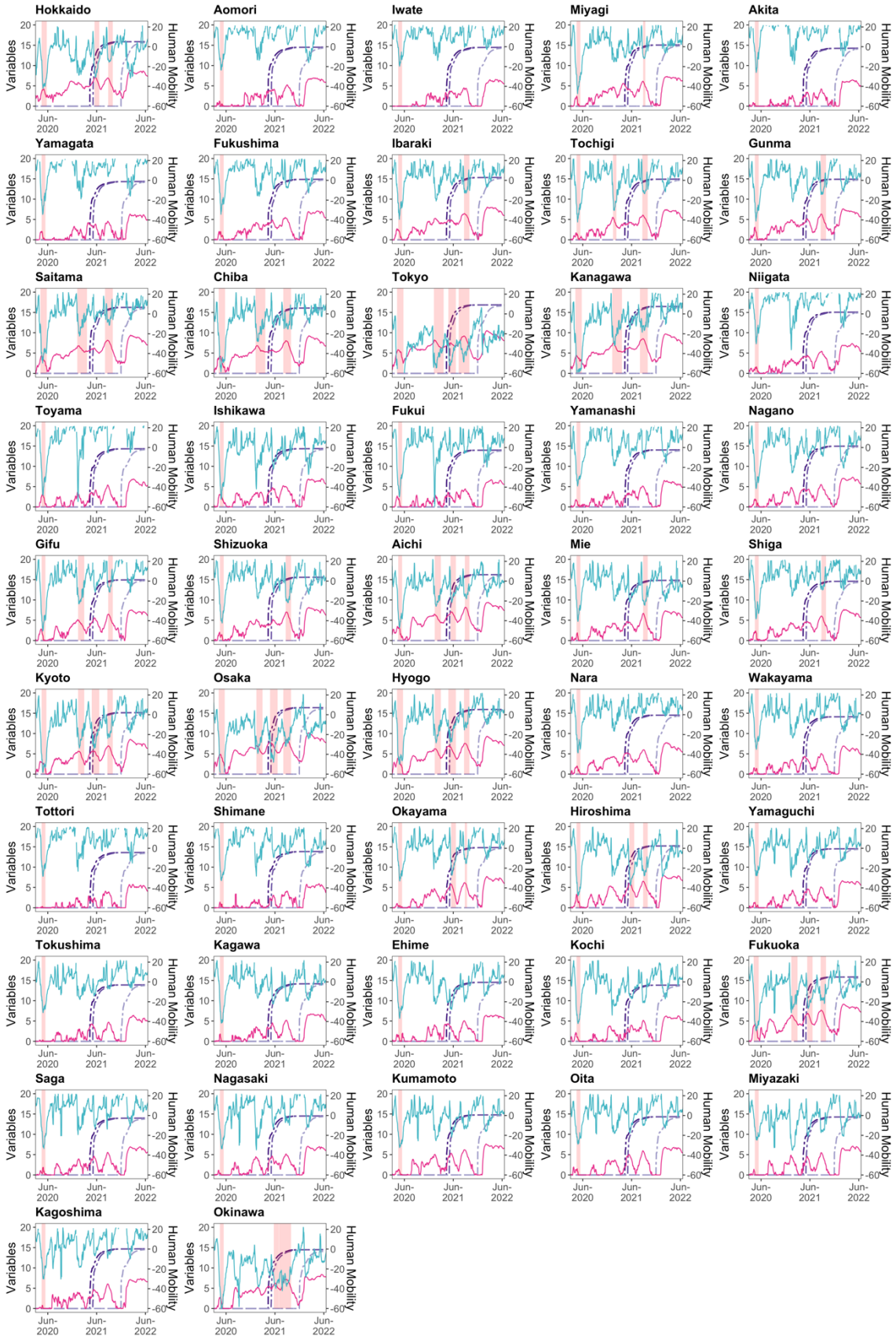
Hokkaido
Aomori
Iwate
Miyagi
Akita
Yamagata
Fukushima
Ibaraki
Tochigi
Gunma
Saitama
Chiba
Tokyo
Kanagawa
Niigata
Toyama
Ishikawa
Fukui
Yamanashi
Nagano
Gifu
Shizuoka
Aichi
Mie
Shiga
Kyoto
Osaka
Hyogo
Nara
Wakayama
Tottori
Shimane
Okayama
Hiroshima
Yamaguchi
Tokushima
Kagawa
Ehime
Kochi
Fukuoka
Saga
Nagasaki
Kumamoto
Oita
Miyazaki
Kagoshima
Okinawa
Variables
Human Mobility
Jun-2020
Jun-2021
Jun-2022

**Figure 2.** Time series plots of the variables per prefecture used in the estimation. On each chart, the blue-green-coloured line (on the right-hand axis) is the 7-day backward moving average using the geometric mean of human mobility in retail and recreation; the red-purple-coloured line is the IHS transformation of the 7-day backward moving average number of infected persons; the purple-coloured double-dashed lines are the IHS transformation of the cumulative number of people vaccinated with 1–3 doses, and the pink-shaded areas are the DSE periods. The data transformation employed here, such as the 7-day backward moving average, is only for visualisation purposes; we use other transformations in our estimation.

### *2.6 Spatial weight*

To construct a spatial weight matrix, we acquire a dataset called Cross-Prefecture Travel Data from V-RESAS, a website which contains publicly available information on human mobilities and the economy related to COVID-19 provided by the Cabinet Secretariat and the Cabinet Office, Government of Japan [48]. The details and the construction of the spatial weight matrix, $W_t^* = \sum_{j=1}^{M} w_{ijt}^*$ where $i$ and $j$ ($j = 1, 2, \cdots, M$) are the prefectural indexes, are provided in the Methods section and the Supplementary Information (Appendix E).

During the pandemic, the more people travel from prefecture $i$ to their own prefecture $j$, the more the COVID-19 trend in prefecture $i$ is expected to affect human mobility inside $j$ substantially. Two factors can explain this: (1) the higher the interaction of the people between $i$ and $j$, the higher the risk of COVID-19 transmission across prefectural borders; and (2) for commuters $j$ to $i$, the trends in prefecture $i$ are of concern.

As an example, the elements of the spatial weight matrix for the last week of January 2020 (27 January–2 February 2020) are illustrated in Fig. 3. This period occurred just prior to the pandemic when irregular movements due to the New Year celebrations in Japan had already dissipated; as a result, this week is representative of normal inter-prefecture travel. In Fig. 3, the dark-red-coloured cells indicate that more people travel between prefectures located in or around large cities such as Tokyo, Aichi, Osaka, and Fukuoka.

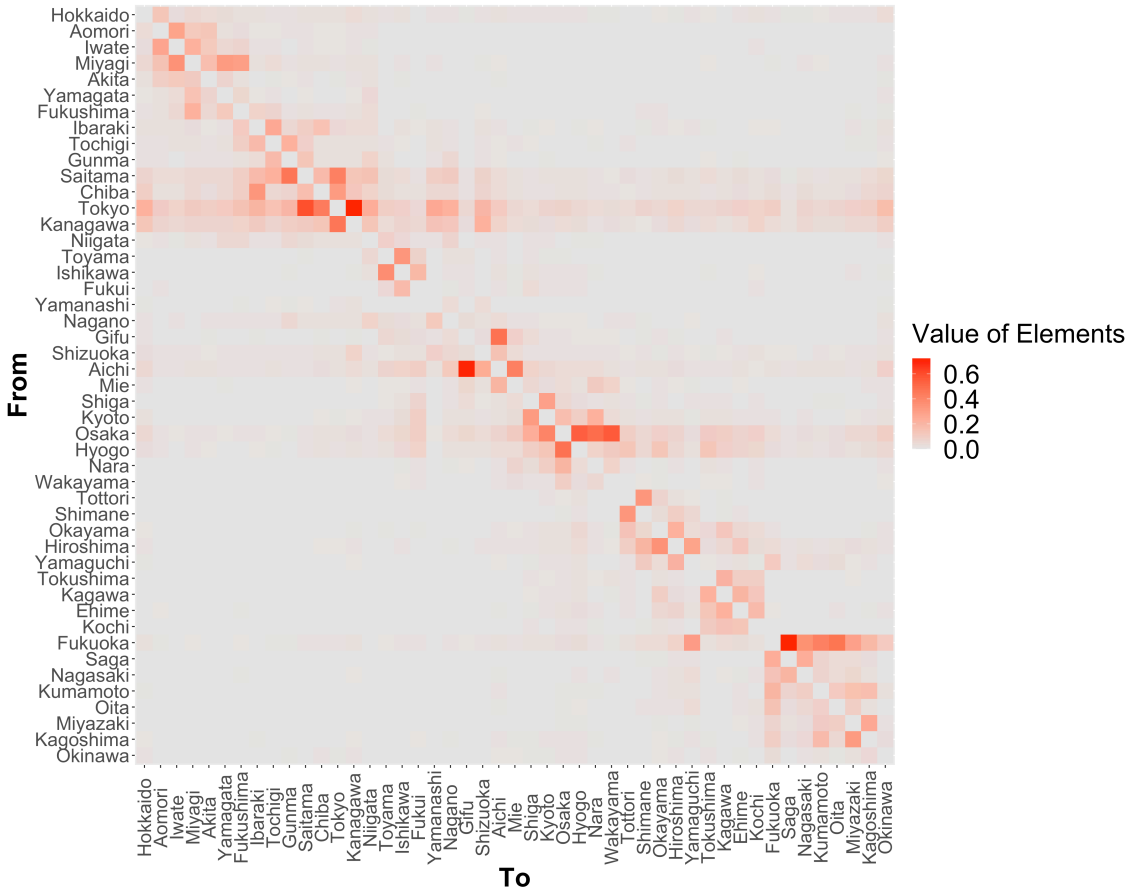


**Figure 3.** Spatial weight matrix per prefecture for the last week of January 2020 (27 January–2 February 2020). Constructed using V-RESAS's Cross-Prefecture Travel data from the Cabinet Secretariat and the Cabinet Office, Government of Japan. Within the figure, the darker the red colour, the greater the number of travellers between prefectures.

### *2.7 Controls*

The Supplementary Information (Appendix F) provides details on the control variables.

### *2.8 Identifying COVID-19 waves*

As the government made no official announcements regarding the beginning and end of COVID-19 infection waves, we independently determine the COVID-19 wave duration of each prefecture, as shown in Fig. 4. Further details are provided in the Supplementary Information (Appendix G).

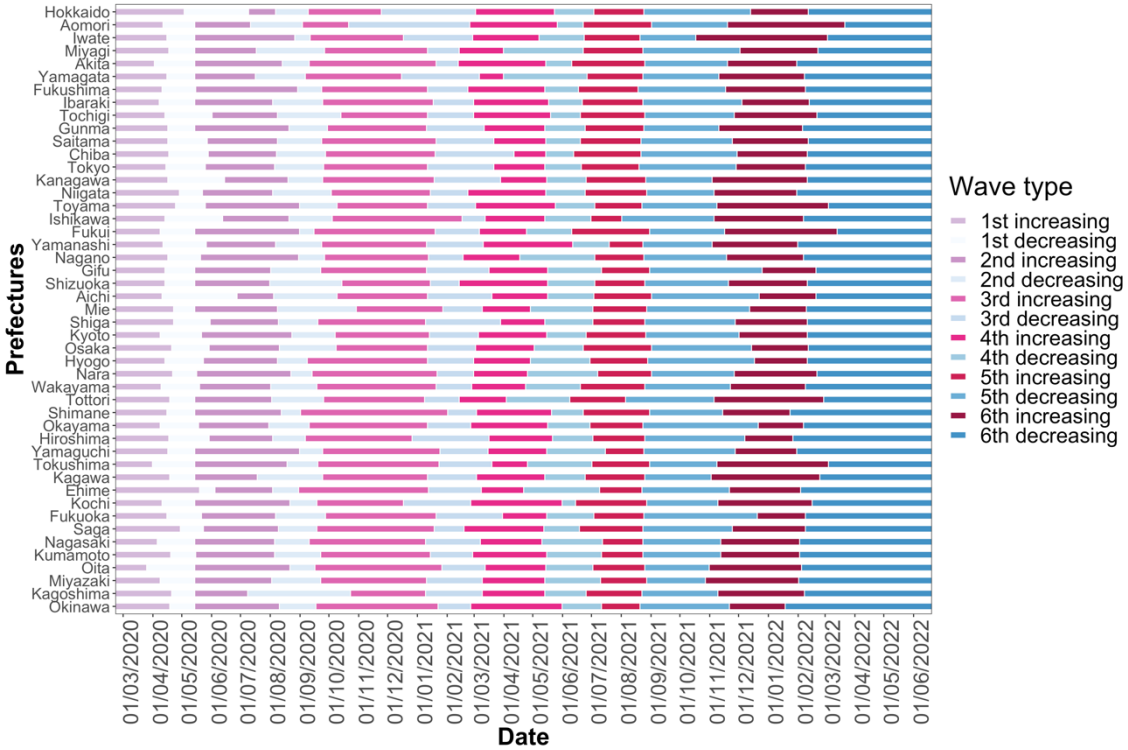


**Figure 4.** COVID-19 wave durations in each prefecture. The data are from 22 February 2020 to 20 June 2022. There are six waves in total, generated by taking a 7-day backward moving average of the number of daily new infections of COVID-19 from NHK.

## 3 Results

The empirical results for human mobility of retail and recreation are presented below.

### *3.1 Empirical approach*

We use the long-term panel data from 47 prefectures over 849 days, from 22 February 2020 to 20 June 2022. Consequently, the total sample size is 39,903. Lags are taken from 1 to 7 days for the week-on-week growth rate of new infections, week-on-week changes in vaccination rate, and the spatially weighted of these variables. Further details of our estimation strategy are provided in the Methods section.

### *3.2 Retail and recreation human mobility response*

#### *3.2.1 Infected cases in the increasing phase*

As shown in Fig. 5a, during the phase of increasing infections, the fear of new infectious diseases substantially reduces human mobility in the first wave. A 1% week-

on-week increase in the number of infected cases results in a decrease in human mobility (which is the percentage change from the baseline) by 1.08-percentage-point (pp) week-on-week, at most (lag: 2, standard error (s.e.) = 0.13). The reduction in human mobility in the first wave weakened daily, from 2- to 7-day lags, as people tend to respond more strongly to the most recent information. The 6- and 7-day lags have a wide confidence interval (95% confidence interval (CI) for lag 7 = [-1.37 to -0.22]), indicating that human behaviours on these lag days after receiving infection information varied widely among prefectures.

The extent of reductions during the second wave is smaller than during the first, but it is still high. Human mobility responses in the second wave also decreased daily, from 3- to 7-day lags, with a maximum 0.70 pp decrease (lag: 3, s.e. = 0.06). The third wave shows a more modest human mobility response than the first and second waves, indicating a tendency towards habituation, with a maximum 0.29 pp decrease (lag: 4, s.e. = 0.08). The response remained flat for each lag day.

In the fourth wave, the Alpha variant became dominant, followed by the Delta variant in the fifth wave and the Omicron variant in the sixth wave [49]. Each new variant exacerbated the speed of infectivity [50], which led to increased fear of the virus. Accordingly, human mobility response rose in the fourth wave. The reduction of human mobility strengthened on lag days 4 and 5, and a maximum week-on-week decrease is 0.49 pp (lag: 5, s.e. = 0.07); people responded to the greatly increasing infected cases continuing for several days.

In the fifth wave, although lag days 1 and 2 do not meet the 5% significance threshold, human mobility is increasingly reduced from the 3- to the 7-day lags to the same degree as in the fourth wave with a maximum 0.38 pp week-on-week decrease (lag: 3, s.e. = 0.16). The response of human mobility in the sixth wave gradually intensified from lag day 1 to 4 and remained significant until lag day 7, with similar reductions as in waves 4 and 5. The maximum week-on-week decrease is 0.42 pp (lag: 4, s.e. = 0.16).

*3.2.2 Infected cases in the decreasing phase*

During the phase of decreasing infection (the recovery phase), as presented in Fig. 5b, if the negative range in the estimated value is large, it indicates a prominent week-on-week increase in human mobility (the percentage change from the baseline), responding to the decreasing infected cases. One explanation is that people become less fearful of

infection in the decreasing phase. Another is that if human mobility decreases greatly during the increasing phase, there is a positive rebound during the recovery phase.

As a result, in the first wave, the negative range is relatively large. However, human mobility remains somewhat reduced, as the magnitudes of the estimates are smaller than those in the increasing phase. A 1% week-on-week decrease in the number of infections will result in, at most, a 0.50 pp (lag: 1, s.e. = 0.13) week-on-week increase in human mobility. In the second wave, the maximum is a 0.35 pp increase (lag: 7, s.e. = 0.04) for week-on-week changes. Only lag 5 is significant at the 5% level for the third wave; however, the estimated coefficient is small.

Early in the pandemic, in 2020 and early 2021, the fear of new infections was presumed to be strong. Our results show smaller magnitudes of human mobility responses in the decreasing phase than in the increasing one, suggesting that people were cautious about the recovery of human mobility, despite habituation trends in the increasing phase. By contrast, the decreasing phase of the fourth wave, in the spring to summer of 2021, shows at most a 0.47 pp (lag: 1, s.e. = 0.05) week-on-week increase in human mobility—a similar magnitude to that of the increasing phase (0.49 pp); it had recovered to the same extent that it decreased during the increasing phase of the fourth wave. This recovery may be due to some positive news about COVID-19 (detailed explanations are provided in the Discussion section). However, in the fifth wave, the estimates are no longer significant, likely because the Delta variant is more transmissible and severe than the Alpha variant [50], making people more fearful of it. Therefore, human mobility did not recover. Finally, the sixth wave shows the highest value of all the waves with a maximum increase of 0.59 pp (lag: 5, s.e. = 0.12). The Omicron variants are more transmissible than the previous ones but are less severe [50]. Therefore, people probably go out more when infections decrease (another explanation for this recovery is probably due to positive news; details are given in the Discussion).

*3.2.3 Spatially weighted infected cases*

The increasing and decreasing phases are not separated for the spatially weighted infected cases (Fig. 5c). We find that individual going-out behaviours dramatically changed in response to infection information from the other prefectures in the first wave. The maximum (in absolute value) is 1.34 pp (lag: 2, s.e. = 0.23), with the confidence interval being wider than that for the results of infected cases of one's own prefecture (Fig. 5a,b). From the second to the fourth wave, the results are insignificant for most lags; the magnitudes are modest for those significant estimates.

Conversely, in the fifth wave, lags 5–7 are significant at the 5% level, with a maximum of 0.38 pp (in absolute value) (lag: 7, s.e. = 0.09). All lags are significant in the sixth wave, with the largest being 0.20 pp (in absolute value) (lag: 3, s.e. = 0.04). The fifth and sixth waves again affected going-out behaviours, possibly from information about infections of the more infectious variants, Delta and Omicron, in other prefectures.

*3.2.4 DSE and spatially weighted DSE*

A DSE was only issued for the first, third, fourth, and fifth waves (Fig. 5d). The first DSE (in the first wave) greatly reduced human mobility. Although the CI is relatively large, we see a 3.48 pp week-on-week decrease (s.e. = 1.37) in the percentage change from the baseline human mobility. Although significant in the second DSE (third wave), the magnitude is low (estimated coefficient (est.) = -0.19, s.e. = 0.02). In the third DSE (fourth wave), the magnitude is large, with a 1.22 pp week-on-week decrease (s.e. = 0.48). The fourth DSE (fifth wave) lead to a slightly lower but still significant, with a 0.55 pp week-on-week decrease (s.e. = 0.14). An interpretation of these results is probably due to the strength of the DSE requests; details are provided in the Discussion section. By contrast, the spatially weighted DSE is not significant in any of the waves, probably because the DSE subject is its own prefecture (Fig. 5e).

*3.2.5 Vaccination and spatially weighted vaccination*

Regarding vaccination, positive estimates are expected because as the vaccination rate increased from the previous week, the more secure people felt going out. As a result (Fig. 5f), for a first vaccine dose, only some lags are significant, with each having a negligible impact. The effect is more apparent for the second than the first dose, which is significant for all lag days. A 1 pp week-on-week increase in the vaccination rate leads to up to 0.22 pp week-on-week increase in the percentage change from the baseline human mobility (lag: 3, s.e. = 0.05). At that time, the public was informed that two vaccine doses would be effective [51]. However, none of the results is significant for the third dose because the timing of the third vaccination varies greatly by person. Spatially weighted vaccination is not significant for any doses (Fig. 5g), possibly because the human mobility of own prefecture is affected only by the vaccination rate of one's own prefecture.

*3.2.6 Controls*

As controls (Fig. 5h), each day and holiday dummy are significant. Additionally, the precipitation coefficient is negative and significant, meaning increased precipitation reduced human mobility.

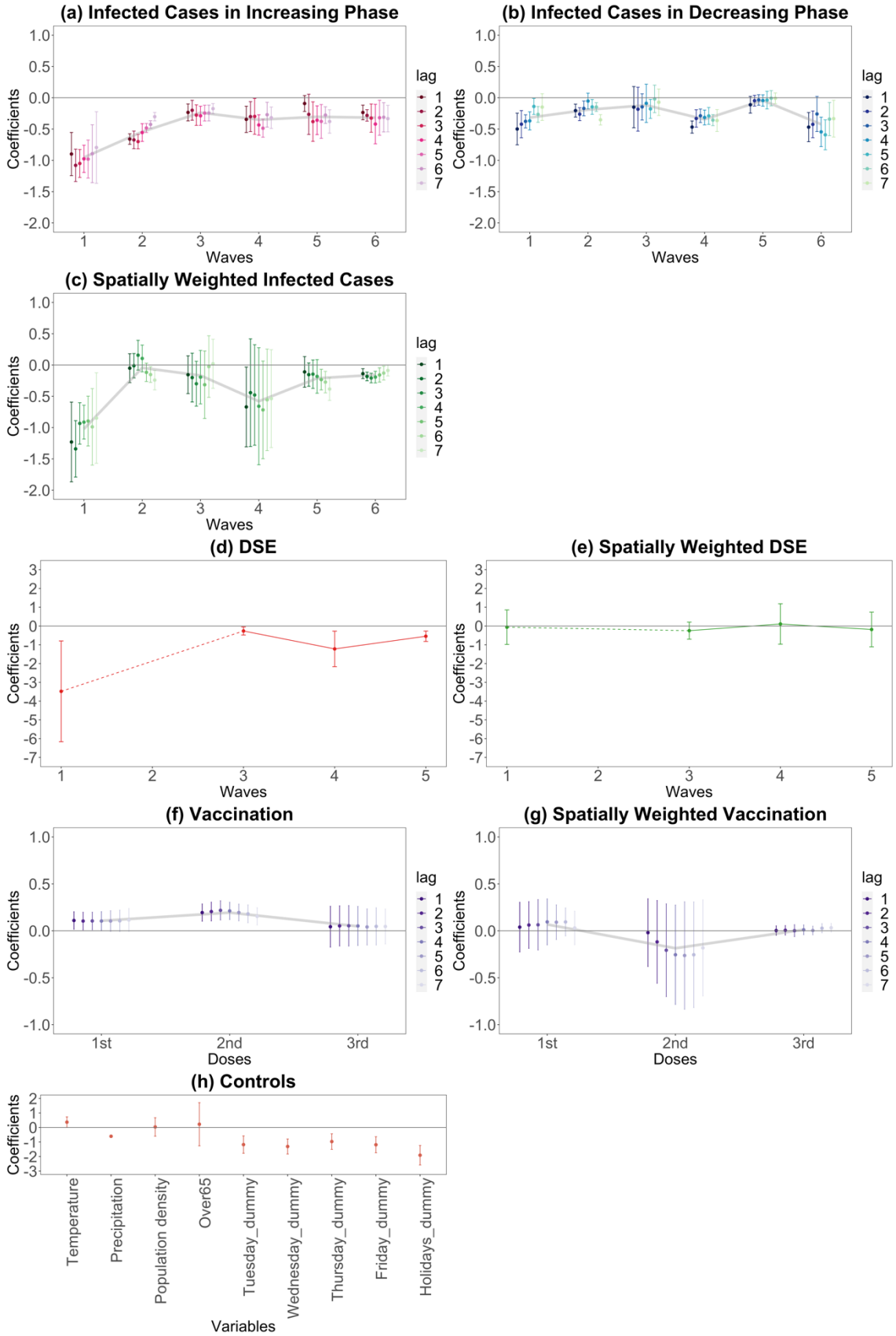
(a) Infected Cases in Increasing Phase
(b) Infected Cases in Decreasing Phase
(c) Spatially Weighted Infected Cases
(d) DSE
(e) Spatially Weighted DSE
(f) Vaccination
(g) Spatially Weighted Vaccination
(h) Controls
Coefficients
Waves
Doses
Variables
lag
1
2
3
4
5
6
7
1st
2nd
3rd
Temperature
Precipitation
Population density
Over65
Tuesday_dummy
Wednesday_dummy
Thursday_dummy
Friday_dummy
Holidays_dummy

**Figure 5.** Retail and recreation human mobility responses to COVID-19-related information. On each chart, the points are estimated coefficients, and the bars indicate upper and lower 95% confidence intervals. The grey line traces the average coefficients of each lag day. There are six infection waves, but DSEs were only issued for the first, third, fourth, and fifth waves. We take a daily lag from 1 to 7 days for infected cases in the increasing phase, infected cases in the decreasing phase, spatially weighted infected cases, vaccination, and spatially weighted vaccination. We conduct the regression analysis seven times, from lags 1 to 7. We do not take a daily lag for the DSE, spatially weighted DSE, and controls; these estimates are from the lag-1 regression.

### *3.3 Robustness*

To test robustness, we conduct the estimation via the polynomial degree 1 Almon lag model of retail and recreation mobility (Fig. 6). As shown in Fig. 6, although vaccination is only significant at the second dose lag-4, the results indicate a similar tendency to our main results. That is, regarding infected cases:

- Habituation in the first to the third waves
- Augmented responses in the fourth to the sixth waves
- Heterogeneity of responses in increasing and decreasing phases
- Lag day trend
- Spatial interactions in the first, fifth, and sixth waves

Regarding DSEs and vaccination:

- Responses of DSEs of own prefecture and second-dose vaccination of own prefecture

In addition, the results of the residential time, which we expect to reflect the opposite impact of that for retail and recreation, are shown in the Supplementary Information (Appendix K) Figs. S3 and S4. These results confirm the robustness of our main results.

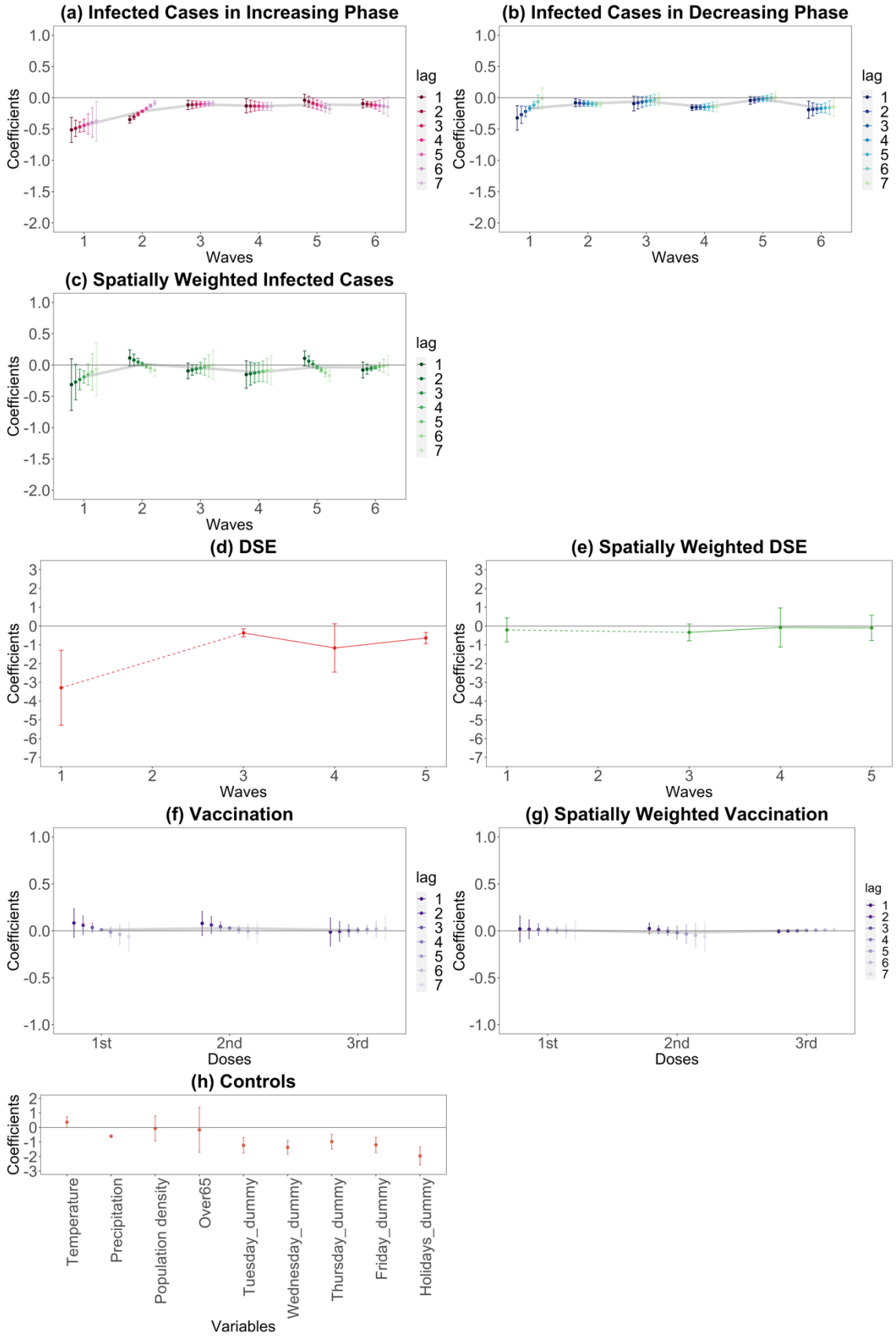
(a) Infected Cases in Increasing Phase
(b) Infected Cases in Decreasing Phase
(c) Spatially Weighted Infected Cases
(d) DSE
(e) Spatially Weighted DSE
(f) Vaccination
(g) Spatially Weighted Vaccination
(h) Controls
Coefficients
Waves
Doses
Variables
lag
1
2
3
4
5
6
7
1st
2nd
3rd
Temperature
Precipitation
Population density
Over65
Tuesday_dummy
Wednesday_dummy
Thursday_dummy
Friday_dummy
Holidays_dummy

**Figure 6.** Retail and recreation human mobility responses to COVID-19-related information using the Almon lag model. On each chart, the points are estimated coefficients, and the bars indicate upper and lower 95% confidence intervals. The grey line traces the average coefficients of each lag day. There are six infection waves, but DSEs were only issued for the first, third, fourth, and fifth waves. We take a daily lag from 1 to 7 days for infected cases in the increasing phase, infected cases in the decreasing phase, spatially weighted infected cases, vaccination, and spatially weighted vaccination. We do not take a daily lag for the DSE, spatially weighted DSE, and controls.

## 4 Discussion

Retail and recreation mobility responses in the increasing (exacerbating) infection phase suggested that, initially, people feared the increase in infection numbers. However, people gradually became accustomed to the new infections over the first three waves. This process can be described as habituation for infection information, in which people become accustomed to similar infection information. However, in the decreasing (recovering) phase, many people remained cautious about COVID-19, and the recovery of their behaviour was only moderate in the decreasing phase of infection.

By contrast, from the fourth to the sixth wave, the Alpha, Delta, and Omicron variants began to dominate, respectively, and the responses of people in the increasing phase, which had declined until the third wave, began to strengthen again. Unlike up to the third wave, where the response weakened daily or remained flat, from the fourth to the sixth wave, the responses tended to intensify from lag day 3 to lag day 5 in each wave. Due to the emergence of new variants, people probably became much more reluctant to go out after receiving information about a growing number of infections for successive days beyond their anticipation. Interestingly, the decreasing phase of infection in waves four and six suggest a prominent recovery of human mobility. These results are probably due to some positive news: the rapid vaccination programme that was promoted [30] and the exposure by people to information regarding COVID-19 post-infection situation and treatment [31, 32] (the sixth wave, as already mentioned, may also be due to a reduction in severity).

As for DSEs, it is more plausible to consider changes in human mobility response as per varying requests rather than habituation (see Supplementary Information, Appendix C, C.1). Thus, since the first DSE (first wave) was a very strong request, it greatly

reduced human mobility. Additionally, the mobility reduction was large in the third DSE (fourth wave), in which the requests were strengthened compared to the second DSE to some extent. In comparison, the magnitudes of the responses in the second and fourth DSEs (third and fifth waves), in which the requests were somewhat mitigated, are low. This result differs substantially from similar studies [24, 25], showing that responses decreased with each DSE. Another possible explanation for the low response in the second DSE was that human mobility was already much lower (before the DSE) in response to the increase in infections at the end of 2020 (e.g. many people cancelled visits to their parents during the New Year holidays [52]). The DSE was issued after the decreasing infections, and human mobility started recovering.

The effect of vaccination is apparent: the second dose led to the recovery of human mobility. At that time, the Japanese government promoted rapid vaccination [30] and released information on the efficacy of the second dose [51]. This is an example of a repeated strong message being vital for effective policy implementation. An effective vaccination programme helps alleviate people's concerns regarding COVID-19 infection and makes them feel safe and secure in public. This reassurance is vital to maintaining economic activity during a pandemic and will benefit the socio-economy.

Our study is the first to demonstrate that responses to information about COVID-19 infection also arise from spatially connected prefectures using prefectural spatial interactions. These responses were substantial for the first, fifth, and sixth waves when the public feared the new infectious disease and its more infectious variants. However, there is no evidence of DSE and vaccination spatial interactions; this is likely because both are only valid in one's own prefecture. This lack of spatial effects is also observed in another study, which finds that the spatial spillover of NPIs to neighbourhoods has only limited effects on human mobility [11].

We acknowledge that this study possesses the following limitations:

1. The data, which are macro data aggregated by prefecture, do not uncover the diversity of behaviours within a prefecture or for each individual.
2. It does not consider policy measures other than emergency declarations, such as semi-state of emergency COVID-19 measures; this remains an issue for future studies.
3. Although data on each variant's infection speed and severity are also crucial for the human mobility response, we cannot incorporate this information into our

model because of the complexity of these spreading mechanisms and the lack of data on people's responses to individual information for each variant.

4. It is impossible to disentangle human mobility recovery into (a) rebound from reduced human mobilities in the increasing phase, (b) announcement effect of promoting vaccination, (c) information about COVID-19 symptoms and treatment options, (d) people's habituation, and (e) any other relevant components.

However, the interactive effects model can control for unobservable information in above 3 and 4 to a certain degree.

Even considering the limitations noted above, our results have several key policy implications. To implement a policy to minimise the spread of COVID-19 infections and to maintain economic activities or, otherwise, prepare for future pandemics, we should consider information dissemination given (1) people's habituation, (2) timing, and (3) effective vaccination promotion. While not an enforceable law, the DSEs in Japan had considerably constrained economic activity, particularly for restaurants. However, our results show that people had reacted to infection information in both their own and other prefectures by limiting their going-out behaviours even when a DSE was not issued. Note that [53] shows that, through simulation, vaccination combined with physical distancing can contain infection without the need for stay-at-home measures. As of July 2022, the Japanese government has been promoting vaccination and advancing its coexistence with COVID-19 [54]. Examining policy effects in more detail will be necessary for future EBPM regarding human mobility.

## 5 Methods

### *5.1 Regression model*

Our analysis uses Bai's 'interactive effects model' [43]. Suppose that we have a panel data set in which $\{(y_{it}, X_{it})\}$, $i = 1, 2, \cdots, N$, $t = 1, 2, \cdots, T$; then, the interactive effects model is expressed as follows:

$$Y_{it} = \boldsymbol{X}'_{it}\boldsymbol{\beta} + v_{it},$$

$$v_{it} = \boldsymbol{\lambda}'_i\boldsymbol{F}_t + e_{it}, (1)$$

where $Y_{it}$ is a dependent variable, $X_{it}$ is a $p \times 1$ vector of explanatory variables such that $p$ is the number of explanatory variables, and $\beta$ is a $p \times 1$ vector of the parameters to be

estimated. While $\lambda_i$ is a $d \times 1$ vector of factor loadings that differ for unit $i$, $F_t$ is a $d \times 1$ vector of a common factor that varies over time $t$, and $e_{it}$ is the error term. An unobservable term $v_{it}$ has factor structure $\lambda'_i F_t$ and random part $e_{it}$. The factor structure allows the model to capture unobservable factors and their loadings.

Applying the interactive effects model, our estimation model becomes:

$$\Delta \boldsymbol{y}_t = \alpha + \sum_{s=1}^{6} \beta_{1s} \boldsymbol{s}'_{st} \Delta \boldsymbol{I}_{t-p}^{*increasing} + \sum_{s=1}^{6} \beta_{2s} \boldsymbol{s}'_{st} \Delta \boldsymbol{I}_{t-p}^{*decreasing}$$
$$+ \sum_{s=1}^{6} \gamma_{1s} \boldsymbol{s}'_{st} \boldsymbol{W}_{t-p}^{*} \Delta \boldsymbol{I}_{t-p}^{*} + \sum_{s=1}^{6} \beta_{3s} \boldsymbol{s}'_{st} \boldsymbol{E}_t + \sum_{s=1}^{6} \gamma_{2s} \boldsymbol{s}'_{st} \boldsymbol{W}_t^{*} \boldsymbol{E}_t$$
$$+ \sum_{v=1}^{3} \beta_{4v} \Delta \boldsymbol{V}_{vt-p} + \sum_{v=1}^{3} \gamma_{3v} \boldsymbol{W}_{t-p}^{*} \Delta \boldsymbol{V}_{vt-p} + \boldsymbol{\delta} \boldsymbol{C}_t + \sum_{d=1}^{D} \boldsymbol{\lambda}_d F_{td} + \boldsymbol{\phi} \boldsymbol{W}_t^{*}$$
$$+ \boldsymbol{\varepsilon}_t, (2)$$

where $\Delta \boldsymbol{y}_t$ is an $N \times 1$ ($N = 47$ prefectures) vector of the week-on-week difference in the percentage change from the baseline of human mobility or the residential time on day $t$ (in pp). Variable $\Delta \boldsymbol{I}_t^*$ is an $N \times 1$ vector of the week-on-week difference of new infections transformed by the IHS. This variable approximates the growth rate of new infections compared to the previous week. We separate $\Delta \boldsymbol{I}_t^*$ for the increasing ($\Delta \boldsymbol{I}_t^{*increasing}$) and decreasing ($\Delta \boldsymbol{I}_t^{*decreasing}$) phases. $\boldsymbol{s}_{st}$ is an $N \times 1$ vector of the step dummies, which takes 1 with each corresponding wave, $s = 1, 2, \cdots, 6$.

$\boldsymbol{E}_t$ is an $N \times 1$ vector of the DSE dummy that takes the value of 1 under a DSE and 0 otherwise. Since DSEs were only issued for the first, third, fourth, and fifth waves, the DSE dummies for the second and sixth waves are zero. Variable $\Delta \boldsymbol{V}_{vt}$ is an $N \times 1$ vector of the week-on-week change in the vaccination rate per million persons. Index $v$ denotes the number of vaccine doses (from the first to the third dose) administered.

Here, spatial weight matrices $\boldsymbol{W}_t^* = \sum_{j=1}^{M} w_{ijt}^*$ vary over time $t$, where $w_{ij}$ is an element of the spatial weight matrix with row $i$ (travel from) and column $j$ (travel to), and diagonal element $w_{ii}$ is 0, and represent the weekly time-series changes in the movement of people between prefectures. Therefore, cross-terms $\boldsymbol{W}_t^* \Delta \boldsymbol{I}_t^*$, $\boldsymbol{W}_t^* \boldsymbol{E}_t$, and $\boldsymbol{W}_t^* \Delta \boldsymbol{V}_{vt}$ exhibit the impact of the number of infections, the DSE, and the vaccination rate from other prefectures, respectively. The larger the spatial weight matrix elements are, the larger the impact on its own prefectures; that is, the more travel from the other prefecture,

the more influenced by information from that prefecture. None of the studies that have explored human mobility regarding COVID-19 has considered these spatial interactions.

Term $\boldsymbol{C}_t$ is an $N \times K$ matrix of a control variable, where $K$ is the number of controls. $F_{td}$ represents the common factors of dimension $d$; $\boldsymbol{\lambda}_d$ is an $N \times 1$ vector where $d = 1, 2, \cdots, D$ is the dimension of factors, representing factor loadings with dimension $d$. $\boldsymbol{\phi W}_t^* = \sum_{j=1}^{M} \phi_j w_{ijt}^*$ represents spatially weighted fixed effects [55, 56]. Finally, $\boldsymbol{\varepsilon}_t$ is an i.i.d. (independent and identically distributed) random component vector. $\boldsymbol{\lambda}_d$, $F_{td}$, and $\boldsymbol{\varepsilon}_t$ are unobservable. Parameters $\alpha$, $\beta_{1s}$, $\beta_{2s}$, $\beta_{3s}$, $\beta_{4v}$, $\gamma_{1s}$, $\gamma_{2s}$, $\gamma_{3v}$, $\boldsymbol{\delta}$ ($K \times 1$ vector), and $\boldsymbol{\phi}$ ($M \times 1$ vector) are to be estimated, while the parameters of interest are $\beta_{1s}$, $\beta_{2s}$, $\beta_{3s}$, $\beta_{4v}$, $\gamma_{1s}$, $\gamma_{2s}$, and $\gamma_{3v}$.

In the estimation, reverse causality from the dependent variable ($\Delta \boldsymbol{y}_t$, human mobility within one's prefecture) to the spatial weight matrix ($\boldsymbol{W}_t^*$, human travel between prefectures) is not of concern; since we use the movement from other prefectures to the relevant prefecture to construct the spatial weight matrix, human mobility in one's own prefecture does not directly affect human travel from other prefectures to one's own prefecture.

### *5.2 Spatial weight matrices*

The time dimension of our estimates is days, while V-RESAS's cross-prefecture travel data in each prefecture are expressed in weeks. Therefore, in our estimation, we use spatial weight matrix ($\boldsymbol{W}^*$) for the week corresponding to day $t$ in the analysis, which gives $\boldsymbol{W}_t^*$ (however, the value of the spatial weight matrix does not change per day within the same week). The larger the element of the spatial weight matrix, $w_{ij}^*$, the higher the number of people moving from prefecture $i$ to $j$. Further details on spatial weight matrices are provided in the Supplementary Information (Appendix E).

### *5.3 Lags*

We take lags for the IHS difference (from the previous week) of new infections, $\Delta I_{it}^*$; its spatially weighted variables, $\boldsymbol{W}_t^* \Delta \boldsymbol{I}_t^*$; the week-on-week increased range of vaccination rate per million persons, $\Delta \boldsymbol{V}_{vt}$; and its spatially weighted variables, $\boldsymbol{W}_t^* \Delta \boldsymbol{V}_{vt}$. Daily lag $p$ from day $t$ is taken from 1 day ($p = 1$) to 7 days ($p = 7$). We also take a lag for the spatial weight matrix, $\boldsymbol{W}_t^*$, which corresponds to lag day $t - p$ of the estimation.

During the pandemic, most people decided whether to go out based on information regarding the infection status announced up to the previous day. Therefore, in our estimation, the maximum lag days is set to 7 (more details can be found in the

Supplementary Information, Appendix I). The same is true for vaccination $\Delta V_{it}$, whereby outgoing behaviour is determined by the vaccines administered up to the previous day. By contrast, the lag is not taken for DSE ($E_{it}$), as DSE on the day, rather than the day before, influences outgoing behaviour. Similarly, lags are not taken for the control variables, day-of-the-week dummies, holidays-dummies, temperature, and precipitation, since each is only relevant for human mobility of that day.

Estimates are conducted separately for each lag day: meaning that the estimation is performed seven times. The estimation of the interactive effects model is conducted using the 'phtt' R library with circumstances of R 4.0.5. A model encompassing all lag orders (distributed lag model) is also estimated to ensure robustness. We employ the polynomial degree 1 Almon lag model to avoid multicollinearity arising from the distributed lag model. Further details on the Almon lag model estimation are provided in the Supplementary Information (Appendix J).

### *5.4 Common factors and loadings*

Common factors, denoted by $F_{td}$, are unobservable elements that vary over time and are common for all cross-sectional (prefectural in our case) units. While since each cross-sectional unit (in our case, prefectures) receives a different load from the common factor, $\boldsymbol{\lambda}_d$ describes the difference in loadings. Component $\sum_{d=1}^{D} \boldsymbol{\lambda}_d F_{td_t}$ corresponds to the generalisation of individual-specific and time-specific fixed effects in the panel data analyses; this component can better describe time-varying unobservable elements with different loadings through cross-sectional units than ordinary two-way fixed effects.

In fact, there are unobservable factors affecting human mobility that should be taken into account. For example, suppose a new variant of COVID-19 emerged in a country other than Japan. In that case, it is probable that people in urban areas such as Tokyo and Osaka, which have international airports and large population concentrations, would be more cautious of the outbreak than people in rural areas. Thus, when vigilant of the severity of a new variant infection, people in urban and rural areas will exercise different levels of caution in responding to such information.

Another example of an unobservable factor is how government policies are transmitted. For instance, even if there is an announcement by the Japanese government regarding vaccinations, each prefecture has a different system for promoting vaccinations, so residents in each prefecture (or, more specifically, each municipality, which is the main body promoting vaccinations) will receive the announcement differently. In addition,

people may welcome the rapid vaccination programme announcement more in prefectures with higher infection rates.

In such cases, these pieces of information are either unobservable or difficult to incorporate into the model. Additionally, such information affects all prefectures simultaneously; however, the level of sensitivity differs by prefecture. Therefore, the interactive effects model is a better method for controlling these unobservable factors. In the first example, common factors $F_{td}$ capture the risk of epidemics of the new variants, while the loadings $\boldsymbol{\lambda}_d$ capture differences between prefectures in vigilance against the new variants.

A Hausman-type specification test proposed by [43] is used to determine whether it is appropriate to use the factors or classical two-way fixed effect; the results of all tests support the factor type. Dimension d of factors is chosen by consistent estimation (Bai and Ng, [57]), which also considers the underestimation of the true variance. Our results show that dimension $d = 7$ . For the variance-covariance matrix, we use heteroscedasticity- and autocorrelation-consistent estimators, proposed by Bai [43].

### *5.5 Spatially weighted fixed effects*

The details of spatially weighted fixed effects can be found in the Supplementary Information (Appendix H).

## References


1. Tandon, A. *et al.* Economic impact of COVID-19, implications for health financing in Asia and Pacific. *World Bank Discussion Paper* https://openknowledge.worldbank.org/bitstream/handle/10986/34572/Economic-Impact-of-COVID-19-Implications-for-Health-Financing-in-Asia-and-Pacific.pdf?sequence=6&isAllowed=y (2020).

2. Fujii, D. & Nakata, T. COVID-19 and output in Japan. *Jpn. Econ. Rev.* **72**, 609–650 (2021).

3. World Health Organization. Transmission of SARS-CoV-2: implications for infection prevention precautions. 9 July 2020 (accessed on 28 October 2022) https://www.who.int/news-room/commentaries/detail/transmission-of-sars-cov-2-implications-for-infection-prevention-precautions (2020).

4. Nouvellet, P. *et al.* Reduction in mobility and COVID-19 transmission. *Nat. Commun.* **12**, 1090; https://doi.org/10.1038/s41467-021-21358-2 (2021).

5. Badr, H. S. *et al.* Association between mobility patterns and COVID-19 transmission in the USA: a mathematical modelling study. *Lancet Infect. Dis.* **20**, 1247–1254 (2020).

6. Kubota, S. The macroeconomics of COVID-19 exit strategy: the case of Japan. *Jpn. Econ. Rev.* **72**, 651–682 (2021).

7. Askitas, N., Tatsiramos, K. & Verheyden, B. Estimating worldwide effects of non-pharmaceutical interventions on COVID-19 incidence and population mobility patterns using a multiple-event study. *Sci. Rep.* **11**, 1972; https://doi.org/10.1038/s41598-021-81442-x (2021).

8. Flaxman, S. *et al.* Estimating the effects of non-pharmaceutical interventions on COVID-19 in Europe. *Nature* **584**, 257–261 (2020).

9. Alfano, V. & Ercolano, S. The efficacy of lockdown against COVID-19: a cross-country panel analysis. *Appl. Health Econ. Health Policy* **18**, 509–517 (2020).

10. Glaeser, E. L., Gorback, C. & Redding, S. J. JUE insight: how much does COVID-19 increase with mobility? Evidence from New York and four other U.S. cities. *J. Urban Econ.* **127**, 103292 (2022).

11. Ilin, C. *et al.* Public mobility data enables COVID-19 forecasting and management at local and global scales. *Sci. Rep.* **11**, 13531; https://doi.org/10.1038/s41598-021-92892-8 (2021).

12. Galeazzi, A. *et al.* Human mobility in response to COVID-19 in France, Italy and UK. *Sci. Rep.* **11**, 13141; https://doi.org/10.1038/s41598-021-92399-2 (2021).

13. Fang, H., Wang, L. & Yang, Y. Human mobility restrictions and the spread of the novel coronavirus (2019-nCoV) in China. *J. Public Econ.* **191**, 104272 (2020).

14. Chan, H. F., Skali, A., Savage, D. A., Stadelmann, D. & Torgler, B. Risk attitudes and human mobility during the COVID-19 pandemic. *Sci. Rep.* **10**, 19931; https://doi.org/10.1038/s41598-020-76763-2 (2020).

15. Goolsbee, A. & Syverson, C. Fear, lockdown, and diversion: comparing drivers of pandemic economic decline 2020. *J. Public Econ.* **193**, 104311 (2021).

16. Borkowski, P., Jażdżewska-Gutta, M. & Szmelter-Jarosz, A. Lockdowned: everyday mobility changes in response to COVID-19. *J. Transp. Geogr.* **90**, 102906 (2021).

17. Rafiq, R., Ahmed, T. & Yusuf, S. U. M. Structural modeling of COVID-19 spread in relation to human mobility. *Transp. Res. Interdiscip. Perspect.* **13**, 100528 (2022).

18. Watanabe, T. & Yabu, T. Japan's voluntary lockdown. *PLoS ONE* **16**, e0252468; https://doi.org/10.1371/journal.pone.0252468 (2021).

19. Hosono, K. Epidemic and economic consequences of voluntary and request-based lockdowns in Japan. *J Jpn. Int. Econ.* **61**, 101147 (2021).

20. Pan, Y. *et al.* Quantifying human mobility behaviour changes during the COVID-19 outbreak in the United States. *Sci. Rep.* **10**, 20742; https://doi.org/10.1038/s41598-020-77751-2 (2020).

21. Mendolia, S., Stavrunova, O. & Yerokhin, O. Determinants of the community mobility during the COVID-19 epidemic: the role of government regulations and information. *J. Econ. Behav. Organ.* **184**, 199–231 (2021).

22. Petherick, A. *et al.* A worldwide assessment of changes in adherence to COVID-19 protective behaviours and hypothesized pandemic fatigue. *Nat. Hum. Behav.* **5**, 1145–1160 (2021).

23. Watanabe, T. & Yabu, T. Japan's voluntary lockdown: further evidence based on age-specific mobile location data. *Jpn. Econ. Rev.* **72**, 333–370 (2021).

24. Kurita, K. & Katafuchi, Y. COVID-19, stigma, and habituation: theory and evidence from mobility data. Preprint at *MPRA* https://mpra.ub.uni-muenchen.de/110253/ (2021).

25. Okamoto, S. State of emergency and human mobility during the COVID-19 pandemic in Japan. *J. Transp. Health* **26**, 101405 (2021).

26. Cabinet Secretariat. The state of emergency (in Japanese). (Accessed on 28 October 2022) https://corona.go.jp/emergency/ (2020).

27. NHK. Wave 1–Wave 6 Graph of the number of infected persons (in Japanese). (Accessed on 15 August 2022) https://www3.nhk.or.jp/news/special/coronavirus/entire/ (2022).

28. Cabinet Secretariat. COVID-19 information and resources. (Accessed on 16 August 2022) https://corona.go.jp/en/ (2022).

29. Coelho, C. M., Suttiwan, P., Arato, N. & Zsido, A. N. On the nature of fear and anxiety triggered by COVID-19. *Front. Psychol.* **11**, 581314; https://doi.org/10.3389/fpsyg.2020.581314 (2020).

30. NHK. Government decides on new financial support measures to accelerate vaccination (in Japanese). 25 May 2021 (accessed on 28 October 2022) https://www3.nhk.or.jp/news/html/20210525/k10013049871000.html (2021).

31. World Health Organization. Therapeutics and COVID-19: living guideline. 14 July 2022 (accessed on 28 October 2022) https://www.who.int/publications/i/item/WHO-2019-nCoV-therapeutics-2022.4 (2022).

32. Center for Disease Control and Prevention. Long COVID or post-COVID conditions. 1 September 2022 (accessed on 28 October 2022) https://www.cdc.gov/coronavirus/2019-ncov/long-term-effects/index.html (2022).

33. Ewen, C. & Heidi, L. How bad is omicron? What scientists know so far. *Nature* **600**, 197–199 (2021).

34. Callaway, E. What the latest omicron subvariants mean for the pandemic. *Nature* **606**, 848–849 (2022).

35. Thompson, R. F. & Spencer, W. A. Habituation: a model phenomenon for the study of neuronal substrates of behavior. *Psychol. Rev* **73**, 16–43 (1966).

36. Groves, P. M, & Thompson, R. F. Habituation: a dual-process theory. *Psychol. Rev.* **77**, 419–450 (1970).

37. Rankin, C. H. *et al.* Habituation revisited: an updated and revised description of the behavioral characteristics of habituation. *Neurobio. Learn. Mem.* **92**, 135–138 (2009).

38. Abreu Costa, M., Kristensen C. H., Dreher C. B., Manfro G. G. & Salum G. A. Habituating to pandemic anxiety: Temporal trends of COVID-19 anxiety over sixteen months of COVID-19. *J. Affect. Disord.* **313**, 32–35 (2022).

39. Kondo, K. Simulating the impacts of interregional mobility restriction on the spatial spread of COVID-19 in Japan. *Sci. Rep.* **11**, 18951; https://doi.org/10.1038/s41598-021-97170-1 (2021).

40. Kang, Y. *et al.* Multiscale dynamic human mobility flow dataset in the U.S. during the COVID-19 epidemic. *Sci. Data* **7**, 390; https://doi.org/10.1038/s41597-020-00734-5 (2020).

41. Graham, A., Kremarik, F. & Kruse, W. Attitudes of ageing passengers to air travel since the coronavirus pandemic. *J. Air Transp. Manag.* **87**, 101865 (2020).

42. Changes in mobility pre and post first SARS-CoV-2 vaccination: findings from a prospective community cohort study including GPS movement tracking in England and Wales (Virus Watch). Preprint at medRxiv https://doi.org/10.1101/2021.06.21.21259237 (2021).

43. Bai, J. Panel data models with interactive fixed effects. *Econometrica* **77**, 1229–1279 (2009).

44. Google. COVID-19 community mobility reports. (Accessed on 16 August 2022) https://www.google.com/covid19/mobility/ (2022).

45. NHK. Number of cases of infection by prefecture. special site: COVID-19 (in Japanese). (Accessed on 16 August 2022). https://www3.nhk.or.jp/news/special/coronavirus/data/ (2022).

46. Digital Agency. Open data on the vaccination status of new corona vaccine. (Accessed on 16 August 2022) https://info.vrs.digital.go.jp/dashboard (2022).

47. Statistics Bureau of Japan. Population estimates. (Accessed on 16 August 2022) https://www.stat.go.jp/data/jinsui/.

48. Cabinet Secretariat and the Cabinet Office. V-RESAS (in Japanese). (Accessed on 16 August 2022) https://v-resas.go.jp (2022).

49. Ren, Z. *et al.* Large-scale serosurveillance of COVID-19 in Japan: acquisition of neutralizing antibodies for delta but not for omicron and requirement of booster vaccination to overcome the Omicron's outbreak. *PLoS ONE* **17**, e0266270; https://doi.org/10.1371/journal.pone.0266270 (2022).

50. Kathy, K. Omicron, Delta, Alpha, and more: What to know about the coronavirus variants. 31 August 2022 (accessed on 28 October 2022) *Yale Medicine* https://www.yalemedicine.org/news/covid-19-variants-of-concern-omicron (2022).

51. Ministry of Health, Labour and Welfare. COVID-19 Q&A (in Japanese). (Accessed on 15 August 2022) https://www.cov19-vaccine.mhlw.go.jp/qa/booster/ (2022).

52. Shinkansen platforms deserted, no rush at the end of the year, less than 50% of passengers in non-reserved seats departing from Shin-Osaka (in Japanese). 29

December 2020 (accessed on 28 October 2022) *Mainichi Shinbun* https://mainichi.jp/articles/20201229/k00/00m/040/239000c (2020).

53. Huang, B. *et al.* Integrated vaccination and physical distancing interventions to prevent future COVID-19 waves in Chinese cities. *Nat. Hum. Behav.* **5**, 695–705 (2021).

54. Japan adopts measures against COVID-19 seventh wave. 15 July 2022 (accessed on 28 October 2022) *The Japan Times* https://www.japantimes.co.jp/news/2022/07/15/national/covid19-panel-seventh-wave-proposals/ (2022).

55. Beer, C. & Riedl, A. Modelling spatial externalities in panel data: The Spatial Durbin model revisited. *Pap Reg Sci*, **91**, 299–318 (2012).

56. Miranda, K., Martínez-Ibañez, O. & Manjón-Antolín M. Estimating individual effects and their spatial spillovers in linear panel data models: Public capital spillovers after all? *Spat. Stat.*, **22** 1–17 (2017).

57. Bai, J. & Ng, S. Determining the number of factors in approximate factor models. *Econometrica* **70**, 191–221 (2002).

**Acknowledgements**

The author thanks Takeshi Miura, Yudai Higashi, Dung Luong Anh, Chigusa Okamoto, Yasuharu Ukai, Shigeki Kano, Yuta Kuroda, and Hiroshi Uno for their helpful comments and suggestions. I also would like to thank seminar participants at the Osaka Metropolitan University. Any remaining errors are the author's alone.

**Competing interests**

The author declares no competing interests.

**Funding**

The author gratefully acknowledges financial support from the Japan Society for the Promotion of Science through Grant-in-Aid for Scientific Research (No. 20K13484).